Int. J. Electrochem. Sci., 10 **(2015)** 9539 - 9546

International Journal of
ELECTROCHEMICAL
SCIENCE
www.electrochemsci.org

Short Communication

A Facile One-Pot Method of Fabricating High Density Pt-Graphene Composite Nanosheets for Methanol Oxidation

Ming La[1,2,*], *Xiaojing Li*[3], *Ting Sun*[4], *Lingbo Qu*[1], *Binbin Zhou*[4], *Feng Zhao*[4,*]

[1]College of Chemistry and Molecular Engineering, Zhengzhou University, Zhengzhou 450000, China
[2]College of Chemistry and Chemical Engineering, Pingdingshan University, Pingdingshan 467000, China
[3]College of Chemical and Food Engineering, Zhongzhou University, Zhengzhou 450000, China
[4]College of Chemistry and Chemical Engineering, Anyang Normal University, Anyang 455000, China
[*]E-mail: mingla2011@163.com(M. L.); zhaofeng327@163.com(F. Z.)

Received: 5 July 2015 / *Accepted:* 27 July 2015 / *Published:* 30 September 2015

Graphene nanosheets loading with high density Pt nanoparticles have been successfully fabricated with a facile one-pot method. Firstly, Fe^{2+} was selectively adsorbed onto the surface of grapheme oxide (GO) via the electrostatic attraction with oxygenate groups of GO. Secondly, Fe^{2+} bonded with oxygenate groups of GO as binder adsorbed negatively charged $PtCl6^{2-}$. The high density Pt-graphene composite nanosheets were applied in methanol eletro-oxidation.

Keywords: Graphene nanosheets; Pt nanoparticles; methanol eletro-oxidation

1. INTRODUCTION

Recently, fuel cell has been receiving great attention owning to the depletion of fossil fuel and the increase in environmental pollution. Direct methanol fuel cell (DMFC) has been regarded as a promising future power source, especially for mobile and portable applications, due to the advantages of high energy density, low operating temperature (60~100 °C), and ease of handling liquid fuel [1,2]. In addition, the applications of effective electrocatalysts for catalyzing the methanol oxidation reaction (MOR) with low overpotentials at the anode electrode play crucial roles for their future application. Pt nanoparticles have been attracted a subtle research interest for the most efficient electrocatalysts for the oxidation of methanol thus far [3-6]. However, the amorphous carbon-supported Pt nanoparticles catalyst suffers from some disadvantages. For example, the reported materials still suffer from low

electrocatalytic activity due to the migration, aggregation, and even dissolution of Pt nanoparticles during operation in the real fuel cell electrode [7]. In order to enhance the catalytic activity of Pt-based catalysts, one strategy is to explore novel carbon materials to effectively disperse catalyst particles.

Graphene, an atom-thick two dimensional (2D) material comprising monolayer hexagonal sp2-hybridized carbons, has been attracting tremendous attention due to its fascinating properties, including giant electron mobility [8-10], high thermal conductivity [11], extraordinary elasticity and stiffness [12], and large specific surface area (2630 m^2g^{-1} from theoretical calculations based on single-layer grapheme sheets) [13]. Many studies have been focused on the utilization of graphene in chemical and biological sensors [14-16], energy-storage materials [17], and polymer composites [18]. Recently, the combination of graphene and various nanomaterials as a new kind of hybrid materials has attracted great attention because of the synergistic enhancement in the electronic, catalytic, and optical properties [19, 20]. Until now, hybrid materials have been published consisting of graphene and various nanoparticles, such as metal, metal oxide, and so on [21-25]. Recently, Pt-graphene catalysts have become a hot topic of interest because they are regarded as the most popular and effective electrocatalysts. Wang et al. proposed a Pt-graphene hybrid nanosheet which was rapidly prepared through a one-step microwave-assisted heating procedure [26]. Zhao et al. reported a facile and effective supercritical fluid approach to load Pt nanoparticles on graphene sheets [27]. However, most of the prepared composites are aggregated and have low Pt nanoparticles on the surface of graphene. Moreover, to avoid aggregations of graphene, different stabilizers such as surfactants and polymers are utilized. However, these additives are difficult to be removed completely, thus severely limiting their chemical activity. Therefore, new strategies to synthesize high density Pt-graphene composite nanosheets without using stabilizers are indispensable. In the present work, we reported a facile one-pot method for the fabrication of high density Pt-graphene (HDPG) composite nanosheets without the use of any reductant and stabilizer. The resulting HDPG nanosheets showed excellent ability for enhancement of the methanol oxidation reaction.

2. EXPERIMENTAL

2.1 Chemicals and reagents

Graphite was from obtained Alfa Aesar. H_2PtCl_6, $FeSO_4$, and dimethylfomamide (DMF) were purchased from Shanghai Chemical Factory (Shanghai, China). Unless otherwise stated, other reagents were of analytical grade and were used as received. All aqueous solutions were prepared with Milli-Q water (18.2 MΩ.cm).

2.2 Apparatus

Raman spectra were collected on a Renishaw (Renishaw, United Kingdom) 2000 model confocal microscopy Raman spectrometer with 514.5 nm wavelength incident laser light. X-ray photoelectron spectroscopy (XPS) measurement was performed on an ESCALAB-MKII spectrometer (VG Co., United Kingdom) with Al Kα X-ray radiation as the X-ray source for excitation.

Transmission electron microscopy (TEM) and high-resolution TEM (HRTEM) images were obtained using a TECNAI G_2 high-resolution transmission electron microscope (Holland) with an accelerating voltage of 200 kV and Hitachi H600 electron microscope (Japan) with an accelerating voltage of 100 kV, respectively. X-ray diffraction (XRD) spectra was obtained on a D8 ADVANCE (Germany) using Cu Kα (1.5406 Å) radiation. Electrochemical experiments were performed on a CHI 660 electrochemical analyzer (CH Instruments, Shanghai, China). A conventional three electrode cell was used, including an Ag/AgCl (saturated KCl) electrode as the reference electrode, a platinum wire as the counter electrode, and a glassy carbon electrode (GCE, 3 mm in diameter) as the working electrode.

2.3 Preparation of Pt-graphene composite nanosheets

The graphene oxide (GO) was synthesized from natural graphite powder according to the literature. In a typical synthesis, 1 mL of GO aqueous solution (5 mg/mL) was dispersed into 30 mL of DMF by sonication for 1 h. Subsequently, 100 μL of $FeSO_4$ aqueous solution (50 mg/mL) was added to the solution. After stirring for 0.5 h, 2 mL of H_2PtCl_6 aqueous solution (1% w/w) was added. After stirring for 10 min, the reaction solution was then transferred to a 40 mL Teflon-lined stainless steel autoclave and kept in an electric oven at 180 ^oC for 6 h. The autoclave was then taken out from the oven and left to cool down to room temperature. The black precipitate was collected by centrifugation, washed thoroughly with water.

2.4 Electrocatalytic experiments

The catalyst was separated by centrifugation and washed with ethanol and 1-Methyl-2-pyrrolidinone (NMP) before it was re-dispersed in a mixture of solvents containing NMP and Nafion (5%) (v/v = 1/0.02) to form a 2 mg/mL suspension. Prior to the surface coating, GCE (3 mm in diameter) was polished with 1.0 and 0.3 μm alumina slurry sequentially and then washed ultrasonically in water and ethanol for a few minutes, respectively. For oxidation, the cleaned GCE was dried with a high-purify nitrogen steam for the next modification. A total of 5 μL of HDPG was dropped on the pretreated GCE surface and dried infrared lamp before electrochemical experiments. Cyclic voltammograms (CVs) were obtained by scanning between –0.2 V and 1.0 V *vs* Ag/AgCl at a scan rate of 50 mV/s in N_2-saturated to obtain the active surface area quantitatively. In this calculation, the charge was assumed to be 210 $\mu C/cm^2$, which is estimated from the hydrogen desorption of the Pt surface area.

3. RESULTS AND DISCUSSION

The synthetic procedure of HDPG is presented in Figure 1. In the first step, GO suspension is mixed with a $FeSO_4$ solution. In this process, Fe^{2+} ions are selectively absorbed by the oxygenate groups via the electrostatic interaction. Secondly, the Fe^{2+} layer acts as a guide for the formation of uniform Pt nanoparticles on the GO surface. The morphology of the HDPG was observed by TEM.

The TEM images of HDPG at different magnification are shown in Figure 2A-B. Low magnification TEM image (Figure 2A) shows that small Pt nanoparticles with good size distribution are uniformly distributed on the graphene. We were pleasantly surprised to find that the density of Pt nanoparticles on graphene is very high and the surface of graphene was almost completely covered by Pt nanoparticles. The magnified image (Figure 2B) shows that these Pt nanoparticles have the size of ~ 4-5 nm. The high-resolution TEM (HRTEM) of Pt nanoparticles is shown in Figure 2C. The *d*-spacings of adjacent fringe for Pt is about 0.23 nm, corresponding to the {111} plane of face-centered cubic (fcc) Pt. The corresponding energy-dispersive X-ray (EDX) spectroscopy (Figure 2D) of HDPG shows the peaks corresponding to C, Fe, and Pt elements, confirming the existence of Pt nanoparticless on the surface of graphene. To confirm the effect of Fe^{2+}, Pt-graphene without $FeSO_4$ was prepared under otherwise identical reaction conditions for comparison. As a result, the typical high-density Pt nanoparticles on the surface of graphene were not found in the final products, indicating that $FeSO_4$ shows a positive effect on the formation of high-density Pt nanoparticles probably due to the its adsorption onto graphene surface.

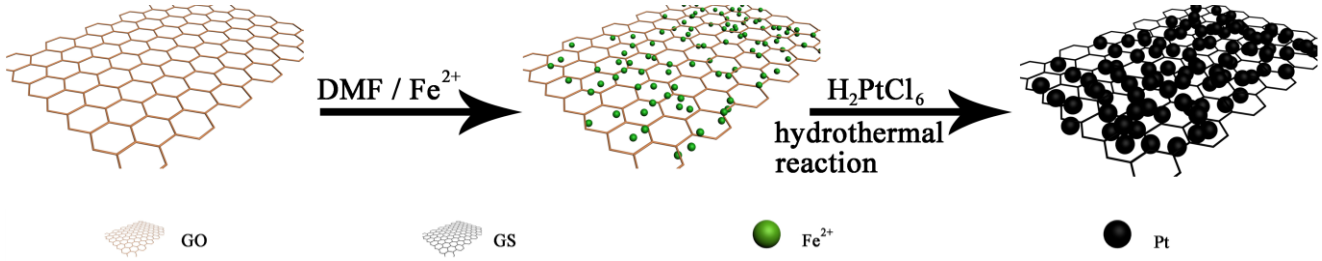

Figure 1. Illustration of the procedure for the preparation of HDPG.

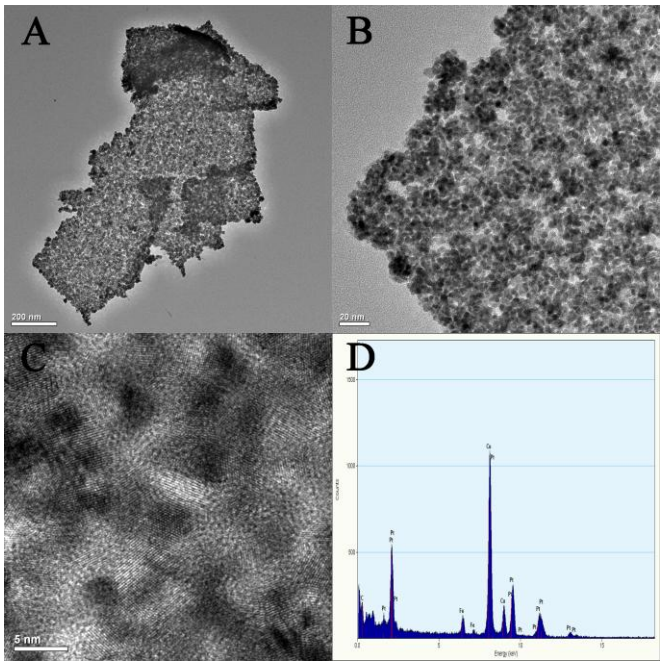

Figure 2. TEM images of HDPG (A, B) at different magnifications. HRTEM image of Pt nanoparticles of HDPG (C). EDX pattern of HDPG (D).

As we known, GO has abundant oxygenate groups on its surface. These functional groups are assumed to be uniformly distributed on the GO surface, which makes the graphene surface with negative charge [28]. When GO suspension was mixed with a $FeSO_4$ solution, Fe^{2+} was selectively bonded with oxygenate groups by the electrostatic interaction. The bound Fe^{2+} in turn can adsorb negatively charged $PtCl_6^{2-}$. Furthermore, DMF was used as both the solvent and the reducing agent in this work. $PtCl_6^{2-}$ was reduced into Pt nanoparticles by the aldehyde group of DMF [29]. To determine the chemical compositions of HDPG, X-ray photoelectron spectroscopy (XPS) measurements were performed in the 0 to 1200 eV range (Figure 3). The survey spectrum (Figure 3A) indicated the presence of carbon, oxygen, platinum and iron, arising from HDPG composite nanosheets. XPS was further used to demonstrate the reduction of GO. Figure 3B shows the C 1s peaks, the peak intensity of oxygen-containing functionalities in the HDPG (Figure 3B, trace 2) is much smaller than that in GO (Figure 3B, trace 1). This observation is indicative of considerable deoxygenation by the hydrothermal treatment. XPS was used to identify the formation of Pt (0) in the synthesized HDPG composite nanosheets. Figure 3C shows the Pt 4f spectrum, and the peaks shown in 71.2 (Pt $4f_{7/2}$) and 74.5 eV (Pt $4f_{5/2}$) provide evidence for the creation of Pt (0) nanoparticles. Figure 3D showed two small peaks at 725 and 711 eV, assignable to Fe $2p_{1/2}$ and Fe $2p_{3/2}$ for Fe_3O_4, respectively. A small number of Fe_3O_4 may come from the high temperature decomposition of $FeSO_4$.

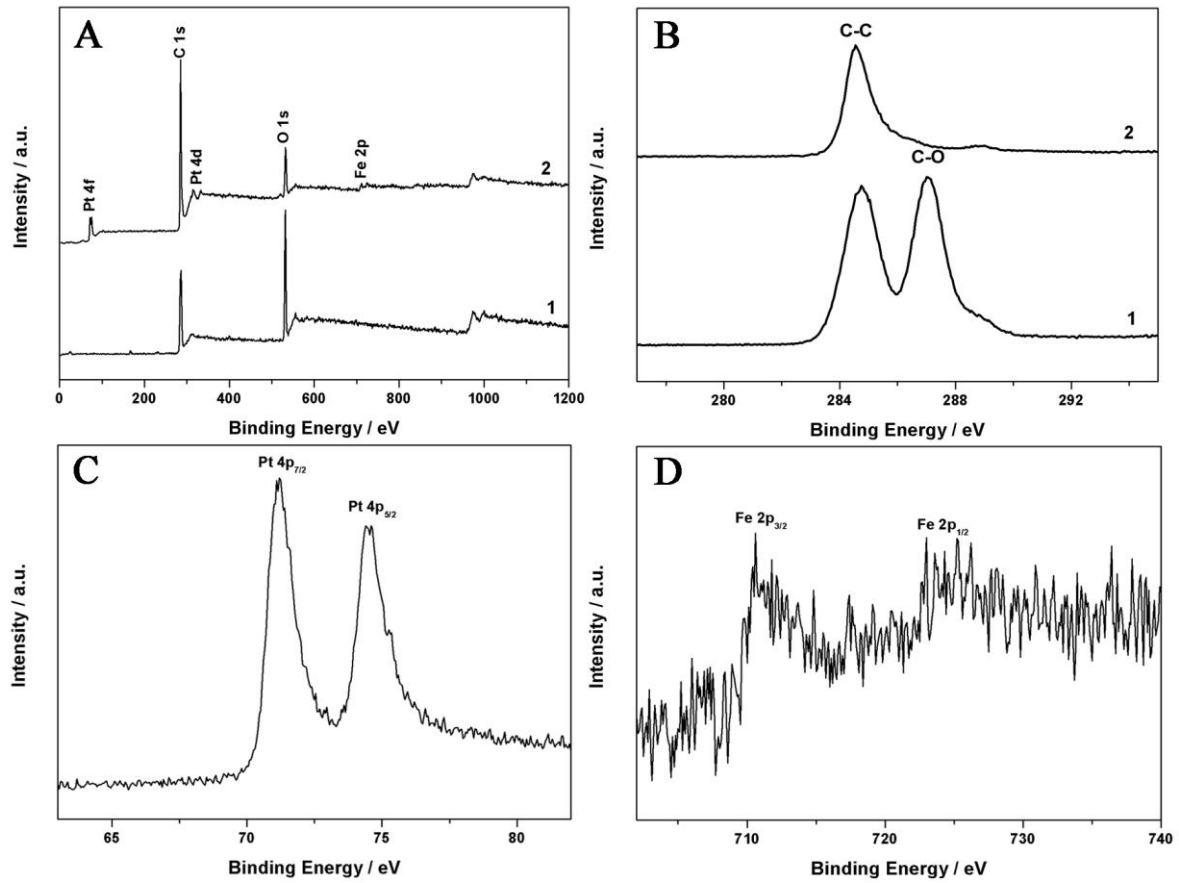

Figure 3. XPS survey spectrum (A) and C1s XPS spectrum (B) of GO (trace 1) and HDPG (trace 2). Pt 4p (C) and Fe 2p (D) XPS spectra of HDPG.

The structural aspects of HDPG were identified by X-ray Diffraction (XRD) pattern (Figure 4). For the pristine graphite (Figure 4A, trace 1), a feature diffraction peak was observed at about 26° (002), corresponding to an interlayer *d*-spacing of 0.34 nm. Compared with pristine graphite, the XRD pattern of graphite oxide (Figure 4A, trace 2) shows a broad and strong diffraction peak at 11.5°, corresponding to the typical diffraction peak of GO nanosheets. For the HDPG, it shows the prominent peaks at 40.1°, 46.6° and 68.1° corresponding to (111), (200) and (220) planes of fcc Pt, respectively (JCPDS cards No 46-1043). Further, a wide and broad peak at 25.5° was observed which is assigned to the (002) plane of graphene. It is interesting to notice that the peak of Fe_3O_4 is not found for the composite. One reason should be that the content of Fe_3O_4 in the composites is relatively low. Raman spectroscopy is a powerful nondestructive technique that has been commonly used to distinguish ordered and disordered crystal structures of carbon. Figure 4B shows the Raman spectra of pristine graphite, graphite oxide and HDPG. Compared to the Raman spectrum of pristine graphite (Figure 4B, trace 1), a broad G band at 1603 cm^{-1} and D band at 1350 cm^{-1} (Figure 4B, trace 2) show the presence of defects within graphite oxide. The ratio between the intensities of the D and G bands (I_D/I_G) is usually used to predict the presence of defects within carbon. After reduction by DMF, it is found that HDPG has an increased I_D/I_G compared to graphite oxide. This change is indicative of a decrease in the size of the in-plane sp^2 domains and a partially ordered crystal structure of HDPG [13].

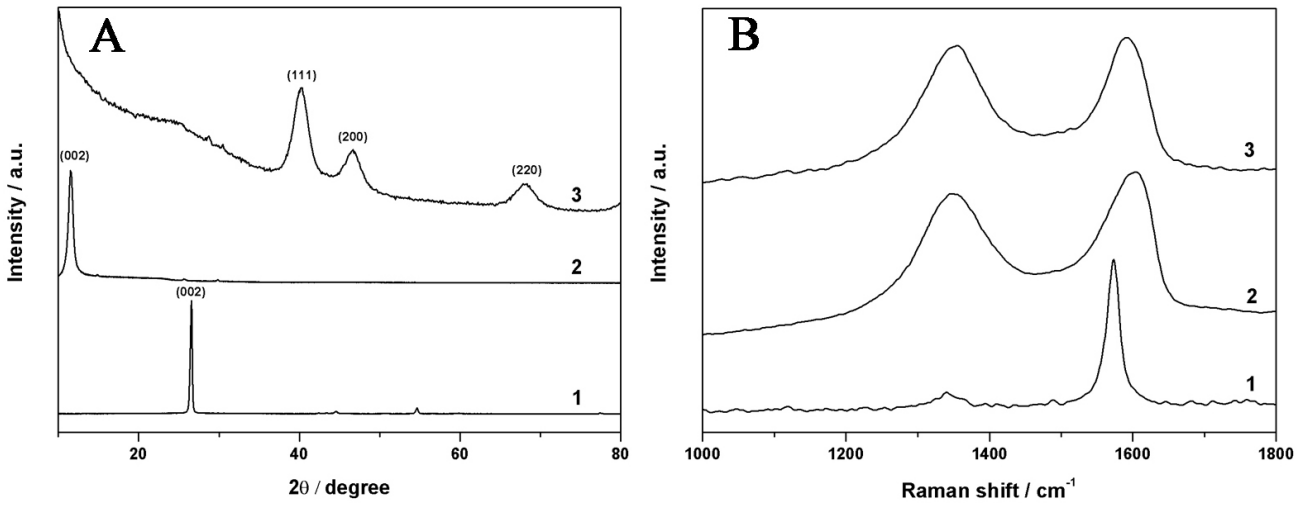

Figure 4. XRD pattern (A) and Raman spectra (B) of pristine graphite (1), graphite oxide (2), and HDPG (3).

The electrocatalytic activity of the HDPG composites for methanol oxidation was studied by electrochemical cyclic voltammetry (CV). The electrochemically active surface area (ECSA) was calculated by using hydrogen adsorption-desorption methods in conjunction with CV and assuming a value of 0.21 mC/cm^2 for the adsorption of a hydrogen monolayer. The ECSA was calculated to be 216 cm^2/mg metal. Figure 5A shows the CV curves for the MOR in a nitrogen saturated solution of 0.5 M H_2SO_4 containing 1 M CH_3OH at a scanning rate of 50 mV/s at room temperature. As shown in Figure 5B, during the positive scan, the current increases until a peak is seen at 0.69 V, which is attributed to electrooxidation of methanol. When the potential scan is reversed, a peak at 0.51 V

occurs, which is due to the reactivation of Pt-oxides. In addition, the ratio of the forward oxidation current peak (I_f) to the reverse current peak (I_b), I_f/I_b, is an important index of the catalyst tolerance to the poisoning of carbonaceous species. A higher ratio of I_f/I_b for HDPG (1.29) indicates more effective removal of the poisoning species on the catalyst surface.

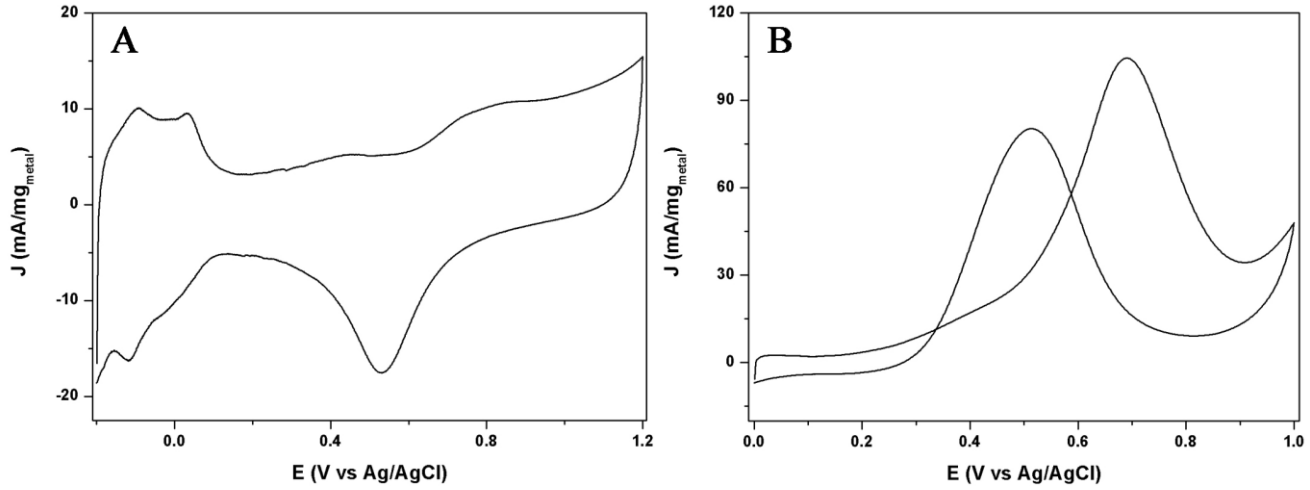

Figure 5. CV (A) of HDPG catalysts in an N_2-saturated 0.5 M H_2SO_4 solution at 50 mV/s. CV (B) for MOR in 0.5 M H_2SO_4 solution containing 1 M CH_3OH at a scan rate of 50 mV/s.

4. CONCLUSION

We have presented a facile one-pot method for the preparation of high density Pt-graphene composite nanosheets. In the synthesis, DMF was used not only as solvent but also as the reducing agent. Fe^{2+} bonded with oxygenate groups of GO as binder can adsorb negatively charged $PtCl_6^{2-}$. The unique structural features are greatly advantageous for enhancement of the MOR. In contrast to other methods for the preparation of Pt-graphene composites, our method obviates the need of additional surfactants, which increased the loading amount of Pt nanoparticles and improved the chemical activity of Pt-graphene composite nanosheets.

ACKOWLEDGMENTS
This work was support by the Project of Education Department of Henan Province (14A150042, 12B430018), the Fund of Department of Science and Technology Department in Henan (KJT142102310462) and the High-Level Personnel Fund in Pingdingshan University (1011014/G).

References

1. J. S. Yu, S. Kang, S. B. Yoon, G. Chai. *J. Am. Chem. Soc.* 124 (2002) 9382.
2. J. N. Zhang, S. J. Guo, J. Y. Wei, Q. Xu, W. F. Yan, J. W. Fu, S. P. Wang, M. J. Cao, Z. M. Chen. *Chem. Eur. J.* 19 (2013) 16087.
3. F. Bai, Z. C. Sun, H. M. Wu, R. E. Haddad, X. Y. Xiao, H. Y. Fan. *Nano Lett.* 11 (2011) 3759.

4. C. Bock, C. Paquet, M. Couillard, G. A. Botton, B. R. MacDougall. *J. Am. Chem. Soc.* 126 (2004) 8028.
5. H. Y. Chou, T. K. Yeh, C. H. Tsai. *Int. J. Electrochem. Sci.* 9 (2014) 5763.
6. J. M. Yoon, J. W. Lee, H. G. Lee, Y. T. Yu. *Int. J. Electrochem. Sci.* 9 (2014) 5690.
7. Z. X. Wu, Y. Y. Lv, Y. Y. Xia, P. A. Webley, D. Y. Zhao. *J. Am. Chem. Soc.* 134 (2012) 2236.
8. K. S. Novoselov, A. K. Geim, S. V. Morozov, D. Jiang, M. I. Katsnelson, I. V. Grigorieva, S. V. Dubonos, A. A. Firsov. *Nature* 438 (2005) 197.
9. K. S. Novoselov, A. K. Geim, S. V. Morozov, D. Jiang, Y. Zhang, S. V. Dubonos, I. V. Grigorieva, A. A. Firsov. *Science* 306 (2004) 666.
10. Y. B. Zhang, Y. W. Tan, H. L. Stormer, P. Kim. *Nature* 438 (2005) 201.
11. A. A. Balandin, S. Ghosh, W. Z. Bao, I. Calizo, D. Teweldebrhan, F. Miao, C. N. Lau. *Nano Lett.* 8 (2008) 902.
12. C. Lee, X. D. Wei, J. W. Kysar, J. Hone. *Science* 321 (2008) 385.
13. M. D. Stoller, S. J. Park, Y. W. Zhu, J. H. An, R. S. Ruoff. *Nano Lett.* 8 (2008) 3498.
14. C. H. Lu, H. H. Yang, C. L. Zhu, X. Chen, G. N. Chen. *Angew. Chem. Int. Ed.* 48 (2009) 4785.
15. N. Xia, Y. Gao. *Int. J. Electrochem. Sci.* 10 (2015) 713.
16. N. Xia, L. Zhang. *Materials* 7 (2014) 5366.
17. H. L. Wang, H. S. Casalongue, Y. Y. Liang, H. J. Dai. *J. Am. Chem. Soc.* 132 (2010) 7472.
18. M. A. Worsley, P. J. Pauzauskie, T. Y. Olson, J. Biener, J. H. Satcher, T. F. Baumann. *J. Am. Chem. Soc.* 132 (2010) 14067.
19. Z. Zhang, H. H. Chen, C. Y. Xing, M. Y. Guo, F. G. Xu, X. D. Wang, H. Gruber, B. L. Zhang, J. L. Tang. *Nano Res.* 4 (2011).
20. N. Xia, L. Liu, Z. Sun, B. Zhou. *J. Nanomater.* 2015 (2015) 892674.
21. X. M. Chen, G. H. Wu, J. M. Chen, X. Chen, Z. X. Xie, X. R. Wang. *J. Am. Chem. Soc.* 133 (2011) 3693.
22. M. Jahan, Q. L. Bao, J. X. Yang, K. P. Loh. *J. Am. Chem. Soc.* 132 (2010) 14487.
23. K. Jasuja, V. Berry. *ACS Nano* 3 (2009) 2358.
24. H. L. Li, S. P. Pang, S. Wu, X. L. Feng, K. Mullen, C. Bubeck. *J. Am. Chem. Soc.* 133 (2011) 9423.
25. Z. Zhang, W. S. Yang, X. X. Zou, F. G. Xu, X. D. Wang, B. L. Zhang, J. L. Tang. *J. Coll. Interf. Sci.* 386 (2012) 198.
26. S. J. Guo, D. Wen, Y. M. Zhai, S. J. Dong, E. K. Wang. *ACS Nano* 4 (2010) 3959.
27. J. Zhao, L. Q. Zhang, T. Chen, H. Yu, L. Zhang, H. Xue, H. Q. Hu. *J. Phys. Chem. C* 116 (2012) 21374.
28. Z. Zhang, J. H. Hao, W. S. Yang, B. P. Lu, X. Ke, B. L. Zhang, J. L. Tang. *ACS Appl. Mater. Interfaces* 5 (2013) 3809.
29. X. Q. Huang, Y. J. Li, H. L. Zhou, X. F. Duan, Y. Huang. *Nano Lett.* 12 (2012) 4265.